A Multichannel EMG System for Spatial Measurement of Diaphragm Activities

Roman Kusche, *Member, IEEE*, Jan Graßhoff, *Member, IEEE*, Andra Oltmann, and Philipp Rostalski, *Member, IEEE*

***Abstract*—An important aspect of mechanical ventilation is the recognition and quantification of spontaneous respiratory effort. However, a measurement of flows and pressures often used for this purpose is prone to error. A promising alternative is to detect diaphragmatic contractions, directly. A method recently proposed is to acquire the diaphragm electromyography (EMG) signals using surface electrodes. However, this method is often limited by disturbances and electrode placements for some applications in which the patient is moving, such as rehabilitation or breathing training. In this work, we present a novel noninvasive method that addresses these problems. This method is based on a novel dry electrode belt, which can be used to comfortably derive EMG signals from the thorax, in combination with a developed electrical measurement system. The modular multichannel system is capable of simultaneously deriving and digitizing 32 differential EMG channels and sending them to a personal computer (PC). A specific digital signal processing chain allows combining the data into one robust overall signal. In addition, the signals derived from the thorax can be used to obtain information regarding the spatiotemporal propagation of the diaphragm EMG. To verify the functionality, the system is characterized. Subsequently, subject measurements are performed. From these, the spatiotemporal propagation of diaphragm EMG on the thorax can be identified. For better visualization, this propagation is graphically displayed in a 3-D model. In addition, it is shown how the combination of all signals can be used to obtain a robust overall signal that can be used to control ventilators.**

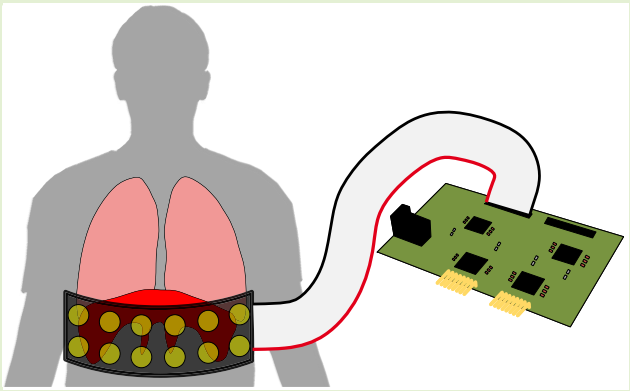

***Index Terms*— Dry electrodes, electrical activity of the diaphragm (EAdi), electrode belt, electromyography, diaphragmatic electromyography (EMGdi), measurement system, multichannel, respiration monitoring, spatiotemporal electromyography (EMG).**

I. Introduction

THE importance of reliable ventilatory support systems and the difficulty of finding appropriate settings for ventilation were demonstrated during the COVID-19 pandemic. In assisted mechanical ventilation modes, which are widely used in most stages of respiratory failure, the patient's spontaneous breathing is superposed by positive pressure support from the ventilator. Both excessive assistance, leading to diaphragmatic fatigue, and insufficient assistance, which is associated with a high level of patient ventilator asynchrony and diaphragmatic injury, should be avoided. Concerning the timing of ventilatory support, it was shown that severe asynchrony is very common and associated with poor outcomes, including increased duration of mechanical ventilation and higher mortality [1], [2]. Thus, several authors have recommended to improve diaphragm health by monitoring the patient's spontaneous breathing effort and adapting the ventilator support, such that an adequate assistance is reached [3], [4]. This new paradigm was termed *diaphragm-protective ventilation* and has been recognized as a crucial step for improving ventilation therapy. To achieve this goal, it is necessary to accurately quantify the respiratory muscle activity at the bedside and intuitively visualize the information.

So far, airway pressure and flow curves shown on the ventilator are usually used to detect spontaneous breathing. While this method is noninvasive and simple, the pneumatic

Manuscript received 22 April 2022; accepted 7 October 2022. Date of publication 18 October 2022; date of current version 30 November 2022. This work was supported in part by the European Union—European Regional Development Fund, in part by the Federal Government and Land Schleswig-Holstein, and in part by the Project "Diagnose- und Therapieverfahren für die Individualisierte Medizintechnik (IMTE)" under Project 12420002. The associate editor coordinating the review of this article and approving it for publication was Dr. Wei Wang. *(Corresponding author: Roman Kusche.)*

This work involved human subjects or animals in its research. Approval of all ethical and experimental procedures and protocols was granted by the Ethics Committee of the University of Lübeck under Application No. 21-020.

The authors are with the Fraunhofer Research Institution for Individualized and Cell-Based Medical Engineering IMTE, 23562 Lübeck, Germany (e-mail: roman.kusche@imte.fraunhofer.de).

Digital Object Identifier 10.1109/JSEN.2022.3213868

measurements tend to be difficult to interpret and may mask profound patient-ventilator asynchrony [5]. As a consequence, the exact timing of patient efforts is often difficult to detect, and a weak respiratory activity may not be recognized at all.

An alternative approach is to detect breathing activity directly at the respiratory muscles [6], [7], [8], [9]. This is done by quantifying the electrical activity of the respiratory muscles, such as the diaphragm and the intercostal muscles. This technique is called electromyography (EMG) and measures the electrical potential field generated by the action potentials of muscle fibers during contraction. The electrical activity of the diaphragm (EAdi) is usually measured invasively by means of a special nasogastric catheter equipped with an array of electrodes, which are positioned close to the crural part of the diaphragm [6], [7]. The filtered and amplified EAdi signal was shown to closely reflect the neural respiratory drive of the patient and was successfully used to detect patient-ventilator asynchrony [10] and respiratory muscle effort [11]. Despite its advantages, EAdi is still not very common in clinics, because it requires special medical expertise, is invasive, and uncomfortable for the patient.

Research results have shown that the EMG signals of the diaphragm can also be derived from the skin surface using electrodes placed on the thorax [9], [12]. Sensitive measuring instruments are capable of detecting the corresponding EMG signal components. Several studies have provided initial evidence, and that diaphragm surface EMG allows to non-invasively detect the timing [13] and amplitude [14], [15] of breathing efforts. The setups used in the past have mostly relied on using a small number of adhesive gel electrodes, i.e., the most common configuration employs two gel electrodes placed bilaterally at the lower costal margin on the midclavicular line [14], [15]. These proposed diaphragmatic surface EMG techniques are suitable for several intensive care applications, especially when the patient is intubated. However, if the patient requires respiratory support while awake or if the spatial characteristics of diaphragm contractions are of interest for rehabilitation or training purposes, several technical challenges occur. For instance, the spatial EMG acquisition requires a precise electrodes placement in the correct anatomical locations. In addition, the EMG signals of interest are not only small but are often in similar frequency ranges as disturbances, caused by motions or other biosignals, e.g., muscle crosstalk and electrocardiography (ECG). As a result of these practical issues, signal processing is challenging, and a further increase in the measurement quality is not expedient. Instead, higher robustness of diaphragm EMG must be achieved for this kind of measurement applications.

Related to these problems, this work focuses onto three research questions.

1) Can additional redundant signals be used to compensate disturbances?
2) Can multiple EMG channels be merged to a useful information regarding timing and strength of diaphragm activities?
3) Is it possible to detect the spatial behavior of the diaphragmatic EMG for diagnostic purposes?

TABLE I
OVERVIEW OF MULTICHANNEL EMG SYSTEMS

System	CH	Diff.	Res.	A /cm²	Centr.	Exp.
Wu 2021 [16]	32	yes	14 bit	4 / CH	no	yes
Brunelli 2015 [17]	32	-	12 bit	5 / CH	no	yes
Delsys Trigno	32	yes	16 bit	10 / CH	no	-
TMSI SAGA	64	no	24 bit	252	-	yes
Venuto 2020 [18]	10	no	16 bit	-	yes	-
Pancholi 2018 [19]	8	yes	24 bit	-	yes	-
Kast 2016 [20]	8	yes	24 bit	60	yes	-

The approach of this work to address these questions is, therefore, to increase signal redundancies and relevance by including multiple spatially distributed measurement channels. The aim is not only to increase robustness but also the additional acquisition of temporal–spatial information regarding the contractions of the diaphragm. For that, we propose a novel multichannel EMG setup, composed of a dry electrode belt, an EMG measurement system, and a specific signal processing.

Since EMG is an established and often used measurement method, several acquisition systems have been published. Also, multichannel measurements have become an often used technique in recent years, even the commercial devices are available. For the intended purpose of this work, a small portable system with at least 16 differentially measured EMG channels is required. The expected weak and noisy signals need to be digitized with a high resolution. For a particularly high flexibility in terms of electrode belt design, the electronic signal acquisition should be on one central device. Table I shows an overview of current multichannel EMG systems. The systems published by Wu et al. [16] and Brunelli et al. [17] as well as the commercially available Delsys Trigno system provide sufficient channels but are based on a modular concept in which each EMG channel consists of electrodes as well as the electronics. These systems are, therefore, not useful for our aimed setup. In contrast, the Twente Medical Systems International BV (TMSI) SAGA system combines the electronics within one single device and provides even 64 EMG channels with a resolution of 24 bits. However, this device has a diameter of 179 mm and is, therefore, not suitable. The works from De Venuto and Mezzina [18], Pancholi and Joshi [19], and Kast et al. [20] do not provide sufficient measurement channels, and in the corresponding publications, the possibility of expanding the systems has not been clarified. It is, therefore, necessary to develop a new EMG system to address the mentioned requirements.

In this manuscript, the challenges of diaphragm EMG acquisition and the system development are described. Afterward, the technical system performance is analyzed, and first, the subject measurements are presented.

In summary, the main contributions proposed in this work are as follows:

1) design of a novel comfortable dry electrode belt;
2) development of a multichannel EMG acquisition system;
3) the signal processing chain for combining several EMG channels to enable robust diaphragm EMG measurements;
4) a novel 3-D interpretation of diaphragm activities.

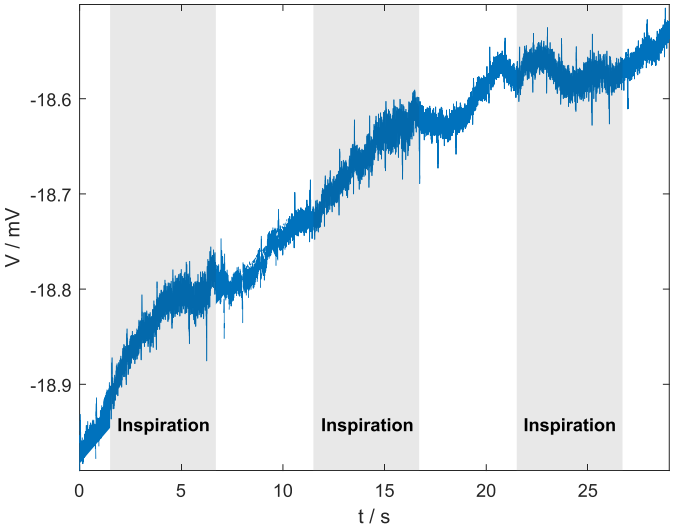

Fig. 1. Exemplary unfiltered differential EMG signal from the upper body during three respiratory cycles.

II. Materials and Methods

A. Challenges of Diaphragm EMG

Although the EMG is a well-known biomedical measurement technique, some technical challenges still exist. One particular difficulty is the electrode contact, which represents the interface between the ionic conduction of the human tissue and the electron conduction of the measurement electronics [21]. Ideally, the resulting electrochemical half-cells have identical and constant half-cell potentials [22]. To create these stable electrode conditions and low contact impedances, adhesive gel electrodes are often used. However, manual placement, contacting, removal, and sometimes allergic reactions motivate the use of dry electrodes, especially for multichannel applications [23]. Unfortunately, the resulting unstable half-cell behavior of the interface between the ion conductor and the electrode conductor can cause temporal changes of the half-cell voltages [24]. Since the electrodes conditions of an EMG channel can be very different, these changes affect the acquired differential voltages. Slow changes can, therefore, cause drifting effects, while fast changes due to motion artifacts or vibrations, as expected in the indented field of applications, generate noise in a higher frequency range. In addition to the half-cell voltages, the high electrode–skin interface impedances reduce the effective common-mode rejection of the measurement setup. This increases the 50/60-Hz noise component in the acquired differential EMG signal [25].

Besides the difficulties caused by the electrodes, the EMG channel itself is technically challenging. On the one hand, the EMG signal amplitudes from the diaphragm are very low in the ranges of some microvolts [14]. On the other hand, the EMG signals have a stochastic behavior mainly between $\approx 20, \ldots, 200$ Hz and are, therefore, difficult to differentiate from motion artifacts in similar frequency ranges [26]. Furthermore, in contrast to measurements at the extremities, dominant ECG signal components are to be expected in measurements on the torso, which are also in a similar frequency range as the EMG [27].

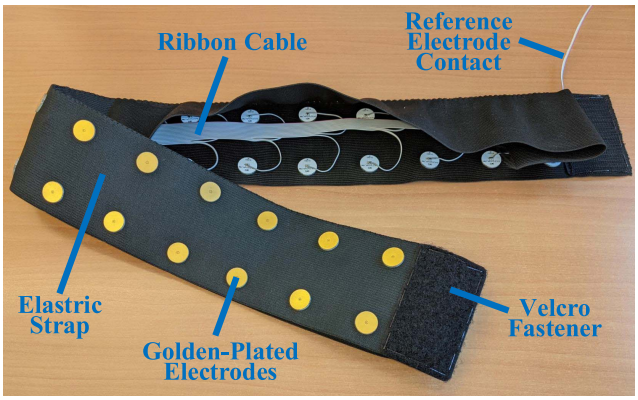

Fig. 2. Flexible dry electrode belt for simultaneous acquisition of 16 differential EMG channels.

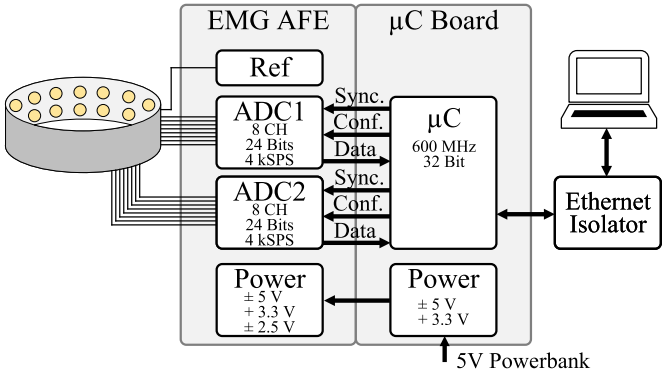

Fig. 3. Block diagram of the 16-channel EMG measurement system.

In Fig. 1, the raw data of a single-channel EMG measurement from the upper body are presented to demonstrate the typical signal conditions. As described, a strong drift of the whole signal can be seen. In addition, the R-peaks from the ECG can visually be detected. The actual diaphragm EMG during the periods of inspiration is almost invisible due to the high noise level.

B. Dry Electrode Belt

As previously described, this measurement approach is based on the usage of dry electrodes. In order to place them easily on the upper body and to press them with constant force onto the skin, an electrode belt was designed. To automatically adjust the length to the circumference of the subject's thorax and to press the electrodes constantly onto the skin, an elastic strap was used, as shown in Fig. 2.

Conductive materials that are chemically stable and easy to clean are particularly suitable for dry electrodes. In the past, gold-plated circuit boards have proven to be especially easy to manufacture [28]. Therefore, 32 such round circuit boards with a diameter of 15 mm each are used to realize 16 differential EMG channels. For easy contacting, a flat ribbon cable is sewn into the belt, which connects all electrodes.

C. EMG Measurement System

The purpose of the measurement system is the simultaneous acquisition of the 16 EMG channels, their digitization, and

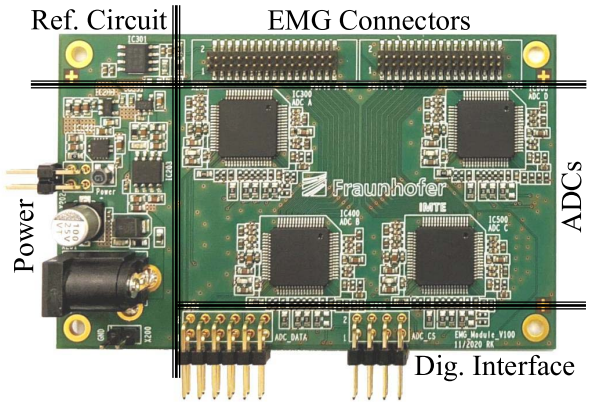

Fig. 4. Photograph of the system's EMG AFE PCB. In this study, only two ADCs with eight channels each are used.

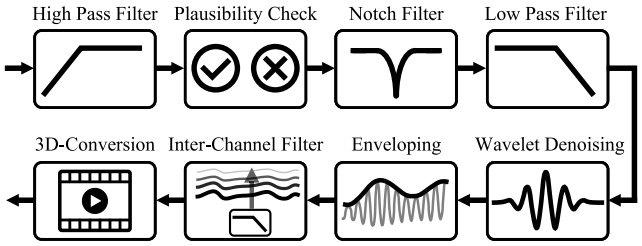

Fig. 5. Block diagram of the major digital signal processing steps. The processing chain is implemented in MATLAB.

subsequent transmission to a personal computer (PC) for signal processing. In order to ensure high flexibility, the system is separated into two parts, as shown in Fig. 3. The analog front end (AFE) is intended to acquire the analog signals from the human body and to digitize them. The task of the microcontroller (μController) board is system configuration and data transmission to a PC.

The AFE contains four analog-to-digital converters (ADC and ADS131E08 from Texas Instruments, Dallas, TX, USA), whereas only two (ADC_1 and ADC_2) are used in this study. Each ADC is capable of digitizing eight differential channels with a resolution of 24 bits simultaneously. The sampling rates can be chosen and are configured to be 4 kSPS. Since the dry electrodes can cause a high measurement sensitivity regarding common-mode voltages, these should be attenuated by applying an active reference voltage to the subject. This voltage is generated by a reference driver circuit (Ref), which inverts and amplifies the common-mode using two operational amplifiers (OPAMP and OPA2134 from Texas Instruments). To ensure the electrical safety, the resulting patient current is limited via a 300-kΩ resistor. The AFE is powered via +5 V from the μController board or another external source. The ADCs require a +3.3 V as well as $\pm$2.5-V power supplies. In addition to the +5-V supply, the OPAMPs are powered via -5 V. Therefore, the input voltage is converted in several steps. For the positive supplies, a switching regulator (TPS63001 from Texas Instruments) is used to generate +3.3 V, followed by a linear dropout regulator (TPS73025 from Texas Instruments) for the +2.5 V.

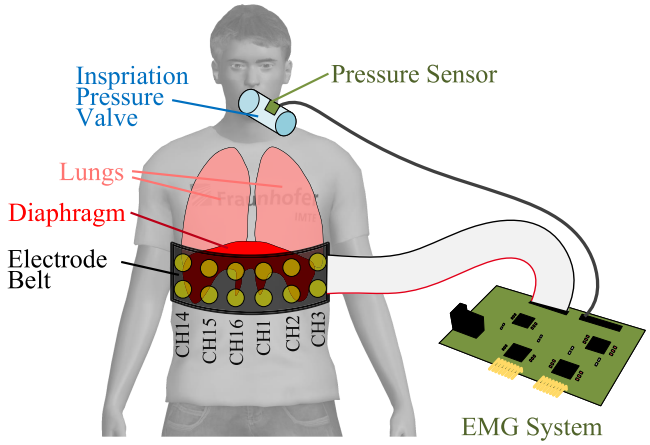

Fig. 6. Measurement setup of the subject study. The subject wears the flexible electrode belt around his thorax. In order to adjust the breathing effort, an inspiration pressure valve is used. The resulting differential pressure and respiration timing are measured via a pressure sensor.

The inverted supplies are realized via a switched-capacitor voltage regulator (ADM660 from Analog Devices, Norwood, MA, USA) in combination with a $-$2.5-V linear dropout regulator (TPS72325 from Texas Instruments).

The μController board is intended to synchronize the ADC components and configure them. In addition, it represents a communication de-/multiplexer that is capable of combining the digitized data of all ADCs to one single Ethernet communication path. To enable a high data throughput, sufficiently large buffers must be available. The chosen μController board is commercially available (Teensy 4.1 from PJRC, Sherwood, OR, USA), based on an advanced RISC machines (ARM) Cortex-M7 controller with a clock frequency of 600 MHz and provides 1 MByte of RAM. It is equipped with a 10/100-Mbps Ethernet PHY transceiver. As shown in the block diagram, this μController board is powered via 5 V. For electrical safety purposes, a powerbank is used for this study. To galvanically separate the measuring system from the PC, a medical Ethernet isolator (MI 1005 from Baaske Medical, Lübbecke, Germany) is used.

A photograph of the developed EMG AFE board is in Fig. 4, which has the dimensions of 86 $\times$ 54 mm. As mentioned above, only two of the visible four ADCs are used in this study, which corresponds to just one EMG connector.

D. Signal Processing Chain

To obtain the EMG signals from the raw data, a signal processing chain is required, as shown in Fig. 5. The implementation is realized in MATLAB (The MathWorks, Natick, MA, USA).

It begins with single-channel operations for each EMG signal. A first-order ($N = 1$) high-pass filter with a cutoff frequency of $f_c = 10$ Hz is implemented to remove the baseline wander. For checking the signal plausibility, which might be affected by electrode lift-offs, the rms values of all channels are calculated and compared with each other. The 50-Hz noise from the mains and its first two harmonics are attenuated via three notch filters ($f_{N1} = 50$ Hz, $f_{N2} = 100$ Hz, and $f_{N3} = 150$ Hz). Afterward, a Butterworth

low-pass filter ($N = 5$ and $f_c = 350$ Hz) removes the signal components in the frequency range higher than that of the expected EMG signals. Since the ECG signal components are in a similar frequency range as the EMG, simple filtering is not beneficial. Instead, an adaptive wavelet denoising approach is chosen, which adapts the filtering characteristics to the individual intervals between the dominant R-peaks of the ECG [29]. In the next step, the envelope of the EMG signal is determined. For that, the signal is rectified and moving average filtered over 0.5 s. In order to remove motion artifacts of single channel and further disturbances, the redundancy of many used EMG channels is utilized. This is implemented by an interchannel low-pass filter (FIR, $N = 3$) for spatial smoothing of the envelopes. For better visualization of the specific spatial–temporal behavior and propagation of the EMG signals at the skin surface, the signals are transformed into a 3-D graphical representation.

E. Subject Studies

All subject studies presented in this manuscript were examined under identical conditions and were approved by the ethics committee of the University of Lübeck (#21-020). First, the male healthy subject is asked to place the electrode belt at the height of the diaphragm, as illustrated in Fig. 6.

For easy orientation, the upper edge of the belt is positioned above the caudal end of the sternum. Since the characteristics of dry electrode contacts change significantly within the first few minutes after applying them to the skin, the measurements begin after 5 min [28], [30], [31].

During all measurements, the subject is asked to use a breathing trainer (IMT from Philips, Eindhoven, The Netherlands) as a valve for defining and regulating the inspiration pressure. To measure the temporal behavior and the breathing effort at the same time as the EMG signals, the breathing trainer is equipped with a pressure sensor (MPX5010DP from NXP, Eindhoven). Its output signal is digitized by one of the unused ADC channels.

III. Results and Discussion

A. System Characteristics

Before performing measurements on human subjects and analyzing them, the technical characteristics of the EMG system are determined. For that, known voltage signals are generated via an arbitrary waveform generator (DG822 from Rigol, Suzhou, China) with a sampling rate of 125 MSPS.

The purpose of the first measurement is to detect the time delays between the channels and the settling times of the used ADCs. Therefore, all 16 EMG channels are simultaneously connected to the waveform generator, which is configured to produce a rectangular signal between ± 1 V. In Fig. 7, the acquired raw signals of all 16 channels are plotted for a duration of 1.75 μs, corresponding to eight samples. Caused by the desired synchronicity of the channels, the 16 plots are difficult to differentiate from each other, and in this representation, they look like a single signal. Accordingly, no channel-dependent delays are to be expected in the subject measurements. In addition, it can be seen that the rising time of the digitized step is below 1 ms, and no oscillations occur.

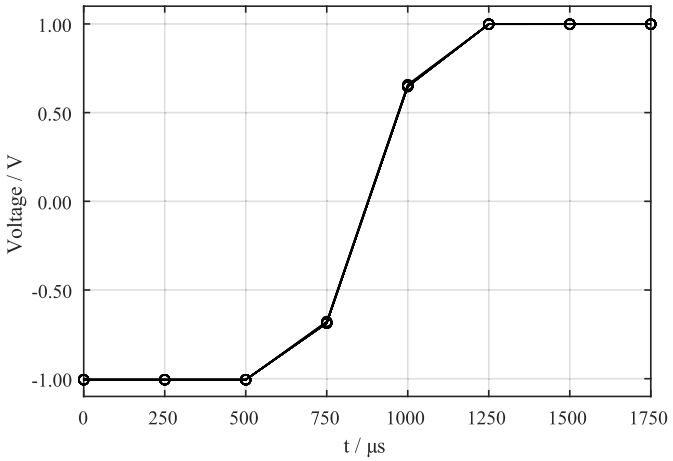

Fig. 7. Measured step responses from −1 to 1 V of all 16 EMG channels. Caused by the synchronous digitization of all channels, timing differences between these 16 plots can hardly be seen.

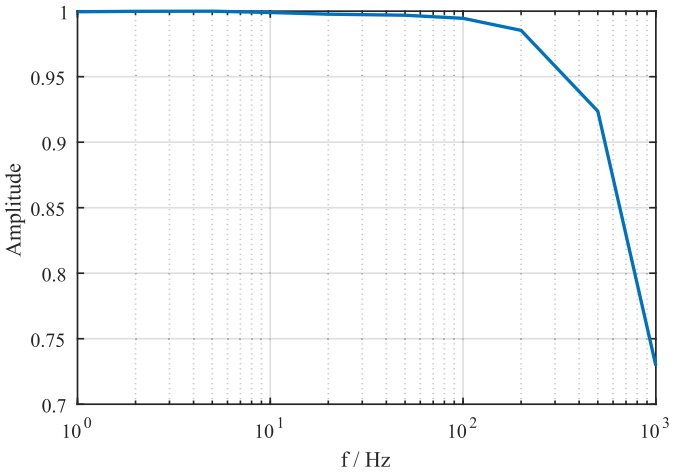

Fig. 8. Measured magnitude response of the EMG channels.

In the second measurement, the magnitude response of the EMG measurement setup is determined. For that, the signal generator is used to generate sinusoidal signals with an amplitude of $\hat{u} = 0.5$ V. The chosen frequencies are $\{1, 2, 5, 10, 20, 50, 100, 200, 500, 1000\}$ Hz. In Fig. 8, the resulting normalized magnitude response is shown. It can be seen that in the typical frequency range, the EMG signals below 200 Hz are attenuated by less than 1.5%.

B. Single-Channel Measurements

Each single EMG signal undergoes several processing steps, as shown above. The focus of this section is to examine the influences of these particular steps. For that, after placing the belt, the subject was asked to lie on his back on a treatment table. In order to generate strong EMG signals during breathing, the inspiration pressure valve threshold was set to $P = 20$ mbar, and the subject was asked to inhale ($T_{\text{in}} = 5$ s) and exhale ($T_{\text{ex}} = 5$ s) deeply for a total duration of 100 s. The acquired raw data of one exemplary channel (CH10) are shown in Fig. 9 (top) for a duration of 28 s.

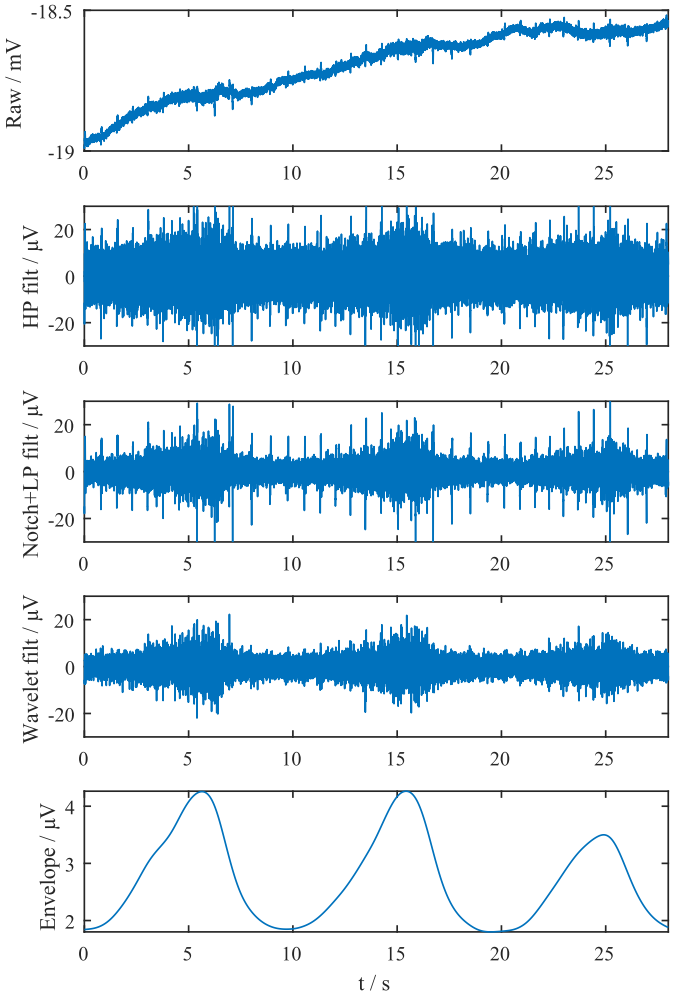

Fig. 9. Exemplary demonstration of the effect of each signal processing step on a single EMG channel.

In the second plot, the result of baseline wandering removal via high-pass filtering is shown. Corresponding to Fig. 5, the next signal processing steps are low-pass and notch filtering, resulting in the signal shown in the middle plot. To remove the very dominant ECG signal components, especially the *R*-peaks, wavelet denoising is applied, leading to a typical EMG signal characteristic. In the last step, the envelope is calculated, as shown in the lowest plot of this figure.

C. Multichannel Measurements

To give an impression of the signal characteristics of all 16 measured EMG channels of the previously described measurement, they are shown in Fig. 10. For better interpretation, the filtered signals are shown here without envelope for their entire duration of 100 s. For temporal orientation, the normalized differential pressure signal from the inspiration pressure valve is plotted below the EMG signals.

In most EMG channels, the times of inhalation are clearly visible. It is also visible that the position of the measurement affects the signal intensity. For instance, in this measurement, the signal amplitudes near the sternum (CH1 and CH16) and the spine (CH8 and CH9) are lower than those at the sides of

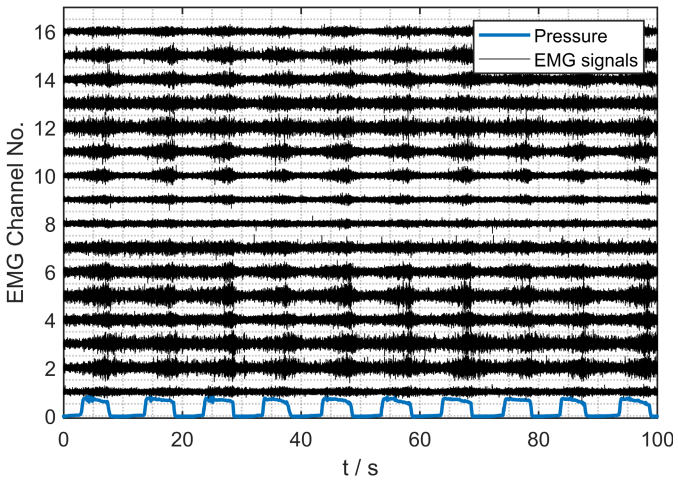

Fig. 10. EMG channels 1–16 during ten respiratory cycles. The time periods of inspiration can be seen in the blue pressure plot below.

the thorax. This distribution is explainable, as in the sternum and spine parts of the body, there is more tissue between the diaphragm and the electrodes. As Lowery et al. [32] demonstrated by means of simulation, this increased distance between source and electrode leads to a stronger attenuation of the signal compared with the sides of the thorax.

D. Spatial Diaphragm EMG

In this section, the behavior of spatial EMG signal propagation is utilized to obtain a graphical representation from it. This could be useful when considering disorders where the activity of the left and right hemidiaphragm is affected. An example of this is unilateral and bilateral diaphragmatic palsy, which results from damage to phrenic nerve or weakness of the diaphragm muscle fibers [33].

In order to obtain the mentioned graphical representation, the envelopes of the signals, shown before in Fig. 10, are calculated, corresponding to the previously presented signal processing chain. Afterward, channel individual disturbances of these envelopes are smoothed via the spatial interchannel low-pass filter. The result of this procedure is shown for one point in time in Fig. 11. In this representation, the normalized values of all 16 envelopes for this specific time are plotted as blue stem charts. The corresponding result of the interchannel filtering is plotted in orange. It can be seen that combining all channels, which are sensitive regarding motion artifacts and further disturbances, results in a reasonable representation with a symmetric behavior and stronger signal components at the thorax sides.

In the next step, the values of the orange plot are visualized on a 3-D model of a human thorax, which was generated via MakeHuman. For this purpose, the different envelope signals were spatially interpolated using a Gaussian process (GP) model. A prior distribution was defined across the 2-D surface using a spatial squared exponential kernel, as described in [34]. The envelope amplitudes were then used as measurements for the GP model, and the potentials at all spatial locations on the geometry were interpolated by calculating the posterior mean of the GP. The resulting image provides an intuitive

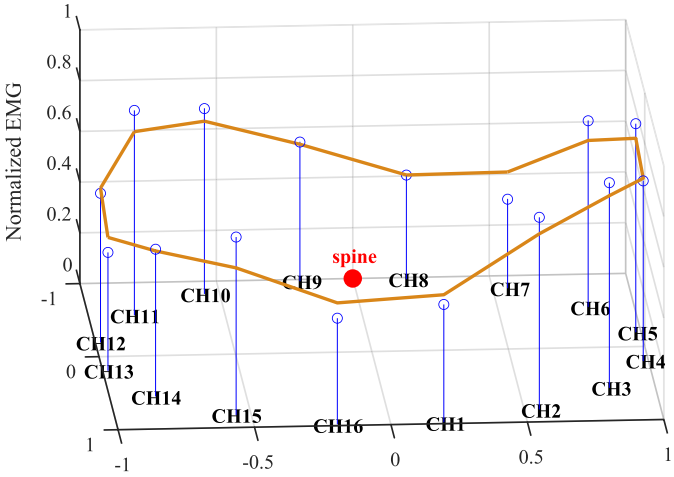

Fig. 11. Representation of all 16 EMG channel envelopes as stem charts at one point in time. The orange plot is the result of averaging adjacent channels.

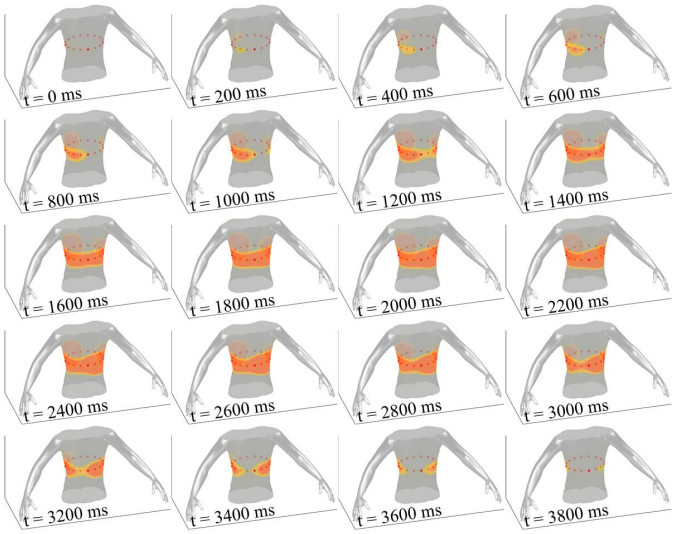

Fig. 12. 3-D representation of the EMG measurement results during inhalation.

insight into the spatial distribution of diaphragmatic activity. The visualization of a time period during inhalation is depicted in Fig. 12 in time steps of 200 ms. At $t = 0$ ms, no electrical activity is visible at the model. In the following plots ($t = 200, \ldots, 1200$ ms), the beginning of EMG activity, especially at the right side from the subject's perspective, is visible. From approximately $t = 1400$ ms until $t = 3000$ ms, the signal intensities of almost all EMG channels reach their maxima. Only the channels close the sternum and to the spine have lower intensities. In the plots of the remaining time steps, an almost symmetrical decrease is visible at both thorax sides.

Since this 3-D representation is based on EMG signals, which passed several steps of filtering, normalization, and graphical conversions, it has to be analyzed carefully. However, it can be useful to combine all information of this kind of multichannel EMG measurement into one visualization. Due to the high sampling rate of the EMG channels, this spatial

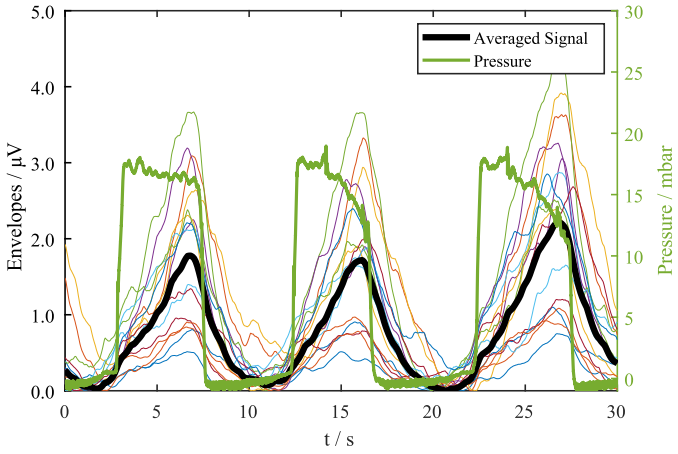

Fig. 13. Envelopes of all 16 EMG signals over three inspiration periods. The bold black plot represents the combined average signal of these envelopes.

behavior can be analyzed in a very high temporal resolution in millisecond ranges or be displayed as a real-time respiration monitor.

E. EMG Channel Merging

In many cases, such as controlling ventilators, it is not the spatial spread of the diaphragm EMG that is of interest but rather a robust overall signal. Based on the previously shown signals, it could already be seen that the exact measurement position has a significant influence on the signal strength and, thus, also on the signal quality. Not only due to inaccurate placement of the electrodes but also due to unpredictable motion artifacts and superposition with other EMG signal components of skeletal muscle groups, no single measurement channel can ensure high robustness. Therefore, in this section, the information from all 16 measurement channels is merged into one signal. As shown in Fig. 13, this is done by averaging the 16 envelopes.

In this diagram, the 16 envelopes of the channels are shown in different colors. The black plot represents the averaged EMG activity at the thorax, and the green signal represents the measured differential pressure that occurs during inhalation. As expected, the averaged signal shows a smoother course than the individual EMG signals. Signal inconsistencies of single channel have almost no effect on the overall signal. It, thus, represents a robust way of measuring respiratory effort for situations in which patient movements have to be considered.

F. Respiratory Effort Dependency

To further analyze the properties of the averaged EMG signal, additional subject measurements were performed. The procedure is analog to the examination described above. The subject wears the electrode belt, lies on his back on a treatment table, and breathes through the inspiration pressure valve. However, in order to consider the influence of the breathing effort on the measured overall signal, the measurement is performed under different threshold configurations of the

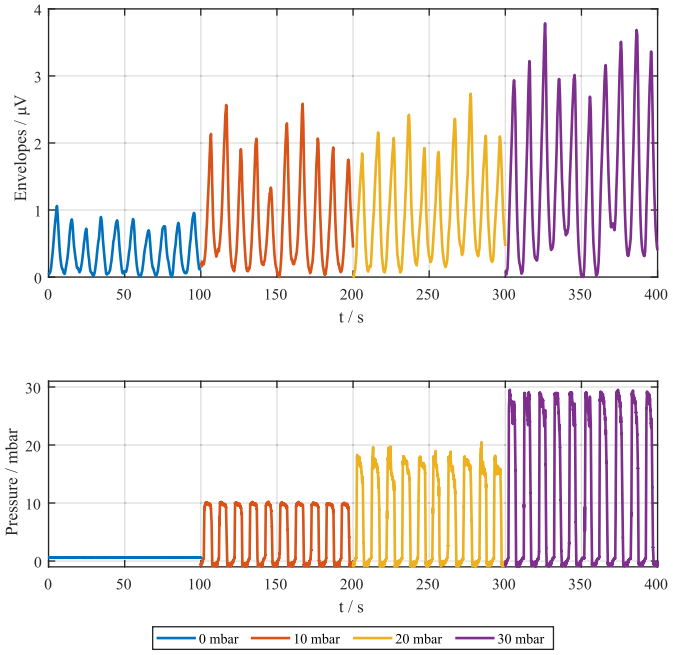

Fig. 14. Top: averaged envelopes for four different configurations of the inspiration pressure valve. Bottom: corresponding measured pressure is plotted. During this measurement, the subject lay on his back.

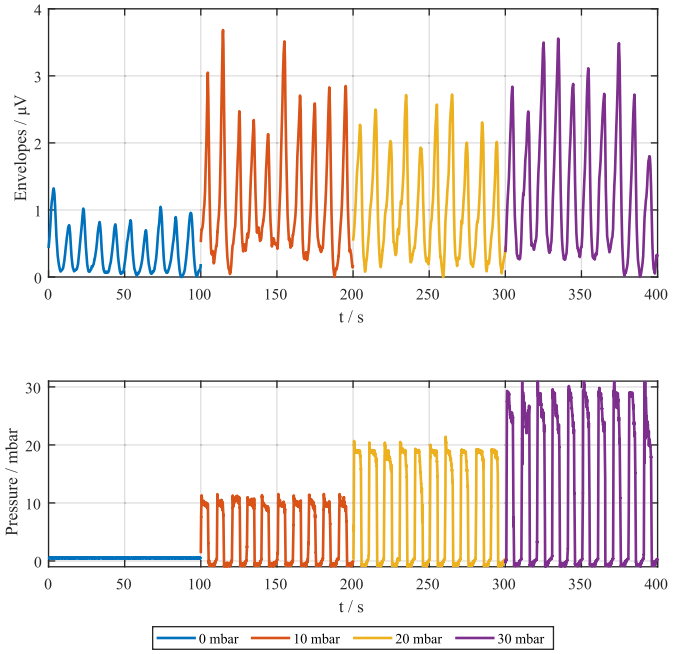

Fig. 15. Top: averaged envelopes for four different configurations of the inspiration pressure valve. Bottom: corresponding measured pressure is plotted. The subject sat on a chair during the measurement.

inspiration pressure valve ($P = \{10, 20, 30\}$ mbar). During the first measurement ($P = 0$ mbar), the pressure valve is omitted. In Fig. 14 (top), the averaged envelopes of the four measurements are shown together and can be distinguished from each other by color. In Fig. 14 (bottom), the corresponding measured pressure signals are shown.

It can be seen that the averaged signals are reliable even at higher respiratory efforts or at lower efforts without using the pressure valve. In addition, a clear correlation between the configured pressures and the respective EMG signal strengths can be recognized. However, in this exemplary measurement, this does not appear to be linear. The difference in amplitude between the time intervals of $P = 0$ mbar and $P = 10$ mbar is significant. The EMG signal strength approximately doubles. However, when comparing the signal strengths of the further pressure increases, almost no further increases of the signal amplitudes can be identified.

This measurement was performed again during sitting on a chair. The obtained results are shown in Fig. 15.

In these measurements, a similar behavior as before can be seen. In this case, however, a reliable estimation of the respiratory effort as a function of the EMG envelope cannot be made if this is above $P = 10$ mbar.

IV. Conclusion

In this work, a novel multichannel EMG system developed to measure the electrical diaphragm activities of awake and moving patients was proposed. For this purpose, a flexible dry electrode belt was presented that is easy to apply and can be used to acquire 16 differential EMG signals from the thorax. Due to the simple connection with only one ribbon cable, neither patient nor medical staff is too much limited in their freedom. By means of a problem-specific signal processing chain, the useful data can be extracted from the signals, which under these particular conditions are often affected by strong disturbances. First examinations in different body positions and under variation of the respiratory effort have shown the functionality and usefulness. On the one hand, the measurement results show the possibility of recording particularly robust EMG signals, as required for the control of ventilators, and, therefore, address the first two research questions in Section I. On the other hand, related to the third research question, the spatial information can also be used to generate a graphical representation of the signal propagation during respiration. This could be used for rehabilitation and training applications or diagnostic purposes in the future. These first results motivate for comprehensive future works. First, extensive subject studies and patient studies would be helpful to analyze, in detail, the relationships between the spatial signal propagation and physiological causes. In addition, the question of the ideal number of measurement channels has not yet been resolved. From the point of view of signal acquisition, it would be advantageous in the future to integrate the measurement electronics and battery into the belt. The connection for data transmission could then be limited to an Ethernet cable or be wireless. If these topics are addressed in the future, many further possible applications are conceivable, for instance, in the field of sports.

References

[1] A. W. Thille, P. Rodriguez, B. Cabello, F. Lellouche, and L. Brochard, "Patient-ventilator asynchrony during assisted mechanical ventilation," *Intensive Care Med.*, vol. 32, no. 10, pp. 1515–1522, 2006.

[2] C. de Haro et al., "Patient-ventilator asynchronies during mechanical ventilation: Current knowledge and research priorities," *Intensive Care Med. Exp.*, vol. 7, Jul. 2019, Art. no. 43.

[3] L. Heunks and C. Ottenheijm, "Diaphragm-protective mechanical ventilation to improve outcomes in ICU patients?" *Amer. J. Respiratory Crit. Care Med.*, vol. 197, no. 2, pp. 150–152, Jan. 2018.

[4] E. C. Goligher et al., "Clinical strategies for implementing lung and diaphragm-protective ventilation: Avoiding insufficient and excessive effort," *Intensive Care Med.*, vol. 46, no. 12, pp. 2314–2326, Nov. 2020.

[5] E. Akoumianaki et al., "The application of esophageal pressure measurement in patients with respiratory failure," *Amer. J. Respiratory Crit. Care Med.*, vol. 189, pp. 520–531, Jan. 2014.

[6] C. A. Sinderby, J. C. Beck, L. H. Lindström, and A. E. Grassino, "Enhancement of signal quality in esophageal recordings of diaphragm EMG," *J. Appl. Physiol.*, vol. 82, no. 4, pp. 1370–1377, Apr. 1997.

[7] C. Sinderby et al., "Neural control of mechanical ventilation in respiratory failure," *Nature Med.*, vol. 5, no. 12, pp. 1433–1436, 1999.

[8] M. L. Duiverman, L. A. van Eykern, P. W. Vennik, G. H. Koëter, E. J. W. Maarsingh, and P. J. Wijkstra, "Reproducibility and responsiveness of a noninvasive EMG technique of the respiratory muscles in COPD patients and in healthy subjects," *J. Appl. Physiol.*, vol. 96, no. 5, pp. 1723–1729, May 2004.

[9] H. Y. AbuNurah, D. W. Russell, and J. D. Lowman, "The validity of surface EMG of extra-diaphragmatic muscles in assessing respiratory responses during mechanical ventilation: A systematic review," *Pulmonology*, vol. 26, no. 6, pp. 378–385, Nov. 2020.

[10] C. Sinderby et al., "An automated and standardized neural index to quantify patient-ventilator interaction," *Crit. Care*, vol. 17, Oct. 2013, Art. no. R239.

[11] G. Bellani et al., "Estimation of patient's inspiratory effort from the electrical activity of the diaphragm," *Crit. Care Med.*, vol. 41, pp. 1483–1491, Mar. 2013.

[12] R. Kusche and M. Ryschka, "Respiration monitoring by combining EMG and bioimpedance measurements," in *Proc. World Congr. Med. Phys. Biomed. Eng.*, L. Lhotska, L. Sukupova, I. Lacković, and G. S. Ibbott, Eds. Singapore: Springer, 2019, pp. 847–850.

[13] A. A. Koopman, R. G. T. Blokpoel, L. A. van Eykern, F. H. C. de Jongh, J. G. M. Burgerhof, and M. C. J. Kneyber, "Transcutaneous electromyographic respiratory muscle recordings to quantify patient–ventilator interaction in mechanically ventilated children," *Ann. Intensive Care*, vol. 8, no. 1, pp. 1–9, Jan. 2018.

[14] G. Bellani et al., "Measurement of diaphragmatic electrical activity by surface electromyography in intubated subjects and its relationship with inspiratory effort," *Respiratory Care*, vol. 63, no. 11, pp. 1341–1349, 2018.

[15] J. Graßhoff et al., "Surface EMG-based quantification of inspiratory effort: A quantitative comparison with P_{es}," *Crit. Care*, vol. 25, Dec. 2021, Art. no. 441.

[16] Y.-D. Wu, S.-J. Ruan, and Y.-H. Lee, "An ultra-low power surface EMG sensor for wearable biometric and medical applications," *Biosensors*, vol. 11, no. 11, p. 411, Oct. 2021.

[17] D. Brunelli, A. M. Tadesse, B. Vodermayer, M. Nowak, and C. Castellini, "Low-cost wearable multichannel surface EMG acquisition for prosthetic hand control," in *Proc. 6th Int. Workshop Adv. Sensors Interfaces (IWASI)*, Jun. 2015, pp. 94–99.

[18] D. De Venuto and G. Mezzina, "Multisensing architecture for the balance losses during gait via physiologic signals recognition," *IEEE Sensors J.*, vol. 20, no. 23, pp. 13959–13968, Dec. 2020.

[19] S. Pancholi and A. M. Joshi, "Portable EMG data acquisition module for upper limb prosthesis application," *IEEE Sensors J.*, vol. 18, no. 8, pp. 3436–3443, Apr. 2018.

[20] C. Kast, M. Krenn, W. Aramphianlert, C. Hofer, O. C. Aszmann, and W. Mayr, "Modular multi-channel real-time bio-signal acquisition system," in *Proc. Int. Conf. Adv. Med. Health Care Through Technol.* Cluj-Napoca, Romania: Springer, 2017, pp. 95–98.

[21] P. F. Shahandashti, H. Pourkheyrollah, A. Jahanshahi, and H. Ghafoorifard, "Highly conformable stretchable dry electrodes based on inexpensive flex substrate for long-term biopotential (EMG/ECG) monitoring," *Sens. Actuators A, Phys.*, vol. 295, pp. 678–686, Aug. 2019. [Online]. Available: https://www.sciencedirect.com/science/article/pii/S0924424719306739

[22] B.-H. Ko et al., "Motion artifact reduction in electrocardiogram using adaptive filtering based on half cell potential monitoring," in *Proc. Annu. Int. Conf. IEEE Eng. Med. Biol. Soc.*, Aug./Sep. 2012, pp. 1590–1593.

[23] Y. Fu, J. Zhao, Y. Dong, and X. Wang, "Dry electrodes for human bioelectrical signal monitoring," *Sensors*, vol. 20, no. 13, p. 3651, Jun. 2020. [Online]. Available: https://www.mdpi.com/1424-8220/20/13/3651

[24] A. Fratini et al., "Muscle movement and electrodes motion artifact during vibration treatment," in *Proc. 14th Nordic-Baltic Conf. Biomed. Eng. Med. Phys.*, A. Katashev, Y. Dekhtyar, and J. Spigulis, Eds. Berlin, Germany: Springer, 2008, pp. 103–106.

[25] E. Spinelli, M. Mayosky, and R. Pallas-Areny, "A practical approach to electrode-skin impedance unbalance measurement," *IEEE Trans. Biomed. Eng.*, vol. 53, no. 7, pp. 1451–1453, Jul. 2006.

[26] I. Mazzetta et al., "Stand-alone wearable system for ubiquitous real-time monitoring of muscle activation potentials," *Sensors*, vol. 18, no. 6, p. 1748, 2018. [Online]. Available: https://www.mdpi.com/1424-8220/18/6/1748

[27] K. J. Lee and B. Lee, "Removing ECG artifacts from the EMG: A comparison between combining empirical-mode decomposition and independent component analysis and other filtering methods," in *Proc. 13th Int. Conf. Control, Autom. Syst. (ICCAS)*, Oct. 2013, pp. 181–184.

[28] R. Kusche, S. Kaufmann, and M. Ryschka, "Dry electrodes for bioimpedance measurements—Design, characterization and comparison," *Biomed. Phys. Eng. Exp.*, vol. 5, no. 1, Nov. 2018, Art. no. 015001.

[29] E. Petersen, J. Sauer, J. Graßhoff, and P. Rostalski, "Removing cardiac artifacts from single-channel respiratory electromyograms," *IEEE Access*, vol. 8, pp. 30905–30917, 2020.

[30] P. Laferriere, E. D. Lemaire, and A. D. C. Chan, "Surface electromyographic signals using dry electrodes," *IEEE Trans. Instrum. Meas.*, vol. 60, no. 10, pp. 3259–3268, Oct. 2011.

[31] J. Muhlsteff and O. Such, "Dry electrodes for monitoring of vital signs in functional textiles," in *Proc. 26th Annu. Int. Conf. IEEE Eng. Med. Biol. Soc.*, vol. 1, Sep. 2004, pp. 2212–2215.

[32] M. M. Lowery, N. S. Stoykov, A. Taflove, and T. A. Kuiken, "A multiple-layer finite-element model of the surface EMG signal," *IEEE Trans. Biomed. Eng.*, vol. 49, no. 5, pp. 446–454, May 2002. [Online]. Available: http://ieeexplore.ieee.org/document/995683/

[33] L. Kokatnur and M. Rudrappa, "Diaphragmatic palsy," *Diseases*, vol. 6, no. 1, p. 16, Feb. 2018.

[34] J. Graßhoff, A. Jankowski, and P. Rostalski, "Scalable Gaussian process separation for kernels with a non-stationary phase," in *Proc. 37th Int. Conf. Mach. Learn.*, H. Daumé, III and A. Singh, Eds., vol. 119, Jul. 2020, pp. 3722–3731. [Online]. Available: https://proceedings.mlr.press/v119/grasshoff20a.html

Roman Kusche (Member, IEEE) received the B.Sc. degree in electrical engineering from the Lübeck University of Applied Sciences, Lübeck, Germany, in 2013, the M.Sc. degree from the Hamburg University of Applied Sciences, Hamburg, Germany, in 2014, and the Ph.D. degree from the University of Lübeck, Lübeck, in 2020.

From 2014 to 2019, he was a Research Group Leader with the Laboratory of Medical Electronics, Lübeck University of Applied Sciences. From 2019 to 2020, he worked as a Senior Researcher with the Center of Excellence CoSA, Lübeck. Since 2020, he has been the Head of the Department for Individulized Therapy, Fraunhofer Research Institution for Individualized and Cell-Based Medical Engineering IMTE, Lübeck. His research interests include development of novel biomedical measurement methods and related medical electronic devices.

Jan Graßhoff (Member, IEEE) received the B.Sc. and M.Sc. degrees in computer science from the Universität zu Lübeck, Lübeck, Germany, where he is currently pursuing the Ph.D. degree.

From 2016 to 2020, he worked as a Research Associate at the Institute for Electrical Engineering in Medicine, Universität zu Lübeck. Currently, he is with the Fraunhofer Research Institution for Individualized and Cell-Based Medical Engineering IMTE, Lübeck, where he is working on novel machine learning techniques for medical devices. His research interests include probabilistic signal processing and parameter/state estimation problems in biomedical applications. In particular, he works on respiratory signal processing and system modeling in the context of mechanical ventilation.

Andra Oltmann received the B.Sc. degree in medical engineering from the Universität zu Lübeck, Lübeck, Germany, in 2017, and the M.Sc. degree in biomedical engineering from the Leibniz Universität Hannover, Hannover, Germany, in 2020.

Since 2020, she has been with the Fraunhofer Research Institution for Individualized and Cell-Based Medical Engineering IMTE, Lübeck. Her research interests include electrophysiological modeling and simulation of human body muscles.

Philipp Rostalski (Member, IEEE) received the Dipl.Ing. degree in electrical engineering with a focus on measurement and control from the Hamburg University of Technology, Hamburg, Germany, in 2004, and the Ph.D. degree from ETH Zürich, Zürich, Switzerland, in 2009.

In 2005, he joined the Automatic Control Laboratory, ETH Zürich, where he worked at the interface of algebraic geometry, optimization, and control. In 2009, he joined the Department of Mathematics, UC Berkeley, Berkeley, CA, USA, as a Feodor Lynen Fellow of the German Alexander von Humboldt Foundation, where he was working on problems in applied mathematics, most notably on convex algebraic geometry. From 2011 to 2015, he was a Research Engineer and the Project Manager of Mechatronics Applications with the Dräger Research Unit, Lübeck, Germany. He was responsible for projects in signal processing and control, with a focus on pneumatic systems and respiratory care. Since 2015, he has been the Director of the Institute for Electrical Engineering in Medicine, Universität zu Lübeck, Lübeck. Since 2020, he has been the Director at the Fraunhofer Research Institution for Individualized and Cell-Based Medical Engineering IMTE, Lübeck.

Prof. Rostalski's Ph.D. thesis was awarded with the ETH Medal for Outstanding Ph.D. theses.